Shaking table tests on seismic earth pressure under large earthquake loads

Tests de table secoueuse sur la poussée sismique des terres sous de fortes charges sismiques

K. Watanabe & M. Tateyama
Railway Technical Research Institute, Japan

ABSTRACT

In order to establish practical design procedure of retaining structure, it is important to evaluate seismic active earth pressure rationally under large earthquake loads. In the current earthquake design procedure, the Mononobe-Okabe theory is often employed to evaluate the seismic active earth pressure. Since this theory is simply derived from method of seismic coefficient, it often derives unrealistic large seismic earth pressure particularly under large seismic load. This often causes practical problems for evaluating seismic stability of retaining structure. To the best knowledge of authors, seismic earth pressure under large earthquake load has not been evaluated sufficiently in the literature. In this study, therefore, a series of shaking table tests were performed, and seismic earth pressure measured on the backface of retaining wall models was compared with M-O theory.

RÉSUMÉ

Il est essentiel d'évaluer rationnellement la poussée sismique des terres pour évaluer la résistance sismique des murs de soutènement. Beaucoup d'études ont été faites dans le passé concernant la poussée sismique des terres agissant contre le mur de soutènement, mais peu en supposant un séisme de grande envergure. Des essais de secousses ayant pour objectif l'évaluation rationnelle de la poussée des terres pendant les gros séismes ont été faits dans cette étude. Dans ces essais, on a mesuré précisément la poussée sismique des terres et l'apparition d'un plan de glissement dans le sol de remblayage. Sur la base des résultats ci-dessus, une méthode de calcul de la poussée sismique des terres s'appliquant aussi aux gros séismes a été proposée, et sa pertinence vérifiée.

Keywords :

1 INTRODUCTION

In recent years, there has been serious damage to retaining walls (RWs) due to large earthquakes. The Hyogoken-Nanbu earthquake on January 17, 1995, for example, caused serious damage to conventional masonry and concrete gravity-type RWs for railway embankments.

After the Hyogoken-Nanbu earthquake, it was suggested that values of the seismic coefficient, $(k_h)_{design}$, used in the current aseismic design procedures should be increased appropriately. In order to establish practical design procedure of retaining structure, it is necessary to evaluate seismic earth pressure rationally under large seismic load.

In the current seismic design procedure, the Mononobe-Okabe (M-O) theory (Okabe 1924; Mononobe and Matsuo 1929) is often used to evaluate the seismic earth pressure (R.T.R.I. 2000). Since this theory is simply based on the pseudo-static approach, it often derives unrealistic large seismic earth pressure particularly under large seismic load. This often causes practical problems for designing retaining structure or evaluating seismic stability of retaining structure.

To the best knowledge of authors, seismic earth pressure under large earthquake load has not been evaluated sufficiently in the literature. In this study, therefore, a series of shaking table tests were performed, and seismic earth pressure measured on the backface of retaining wall models was compared with M-O theory. In addition to this, new image processing system using high speed CCD camera was established to make it possible to measure the dynamic deformation of the backfill soil. The relationship between the seismic earth pressure and the deformation characteristic of backfill was precisely investigated by applying this system to the shaking table tests.

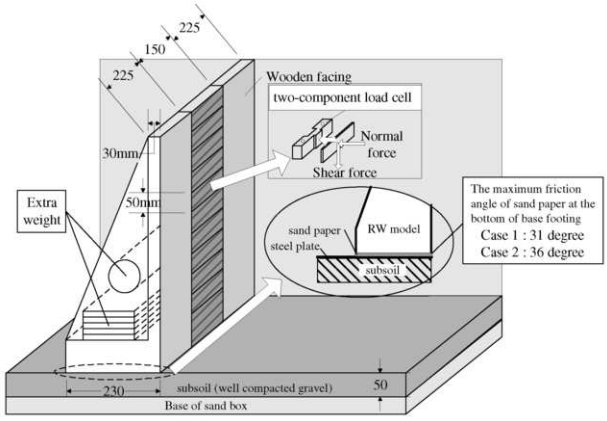

Figure 1. Details of gravity type retaining wall model

2 TESTING PROCEDURE

2.1 *Model of retaining wall and backfill*

Gravity type retaining wall model having 530mm in height was used, and both normal and shear components of seismic earth pressure were monitored using two-components load cells (Fig.1). Backfill model was made of air-dried Toyoura-sand. This model was subjected to large irregular excitation using N-S component of 1995 Hyogoken-nanbu earthquake. Its amplitude and time scale were adjusted so that the base acceleration had

doi:10.3233/978-1-60750-031-5-530

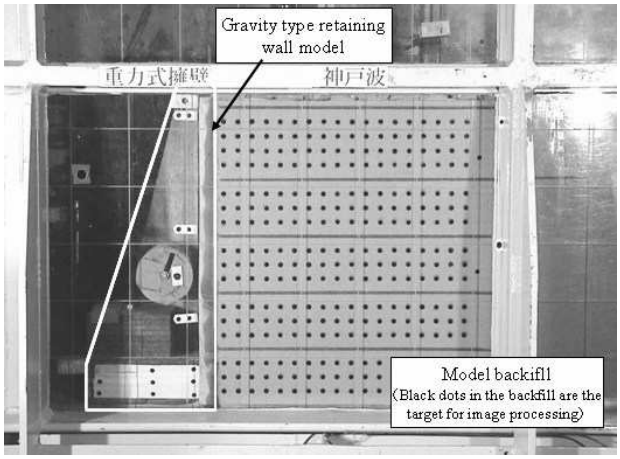

Figure 2. A front view of the model

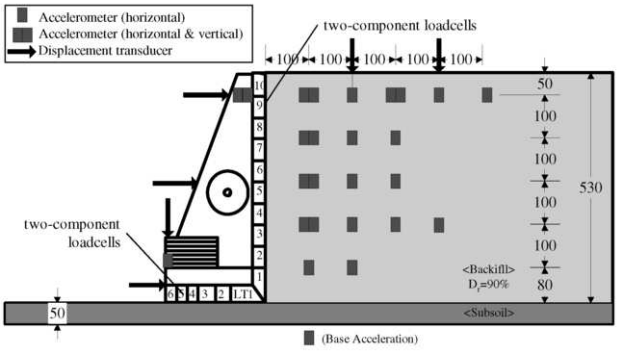

Figure 3. Location of transducers (unit in mm)

the prescribed maximum amplitude (about 935gal) with a predominant frequency of 5Hz. (This predominant frequency is evaluated based on the Fourier spectrum of the base acceleration). The model was subjected to this irregular excitation twice (Case1) or fourth (Case2). Watanabe et al (2003) summarized the detail of the model preparation and the similitude adopted for these shaking table tests.

The subsoil model was made by well-compacted gravel and iron plate which was covered with sand paper was fixed on the subsoil so that the major failure mode of RW becomes lateral sliding (Fig. 1). To study the effect of seismic stability of RW against sliding on seismic earth pressure, the sand paper having larger friction was used to cover the iron plate on the subsoil for Case 2. The maximum friction angle between RW model and iron plate was shown in Fig. 1. This friction angle was obtained by conducting the lateral loading test of RW under static condition.

To observe the deformation of backfill soil visually, horizontal layers of black-dyed Toyoura sand having thickness of 5mm were prepared at a vertical spacing of 100mm adjacent to the transparent side wall of the sand container (Fig. 2). This black-dyed sand is different from the black target for image processing which will be introduced later.

As shown in Fig. 3, a number of displacement transducer and accelerometers were installed to measure the response of RW and backfill. All sensors were placed along the centerline of the wall surface in order to reduce the effect of the sidewall friction of the sand container. The accelerometers in the backfill were mainly arranged inside the soil block by considering where the failure plane supposed to form.

2.2 *Image processing system*

New image processing system using high speed CCD cameras was established to make it possible to measure the two-dimensional deformation of backfill. Two-dimensional movement of the targets set in the backfill soil adjacent to the transparent hard glass sidewall can automatically be measured by this system. A number of rivets made of aluminum with a black circular flat edge were used as targets and they were set in the backfill soil at a horizontal spacing of 25mm and vertical spacing of 25mm or 50mm (Fig. 2). In order to ensure a permanent contact between the glass and the targets, thereby following the surrounding sand movement, silicon grease was smeared between the targets and the glass. Watanabe et al (2005) have summarized the detail of this image processing system.

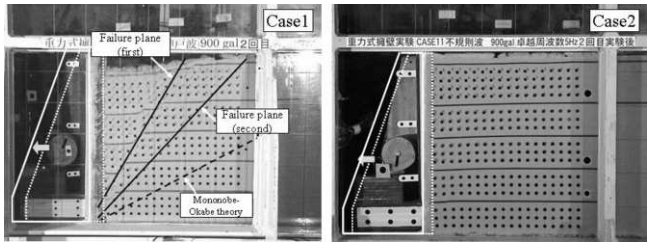

Figure 4. Residual displacement of wall and formation of failure plane (at the end of second shaking test)

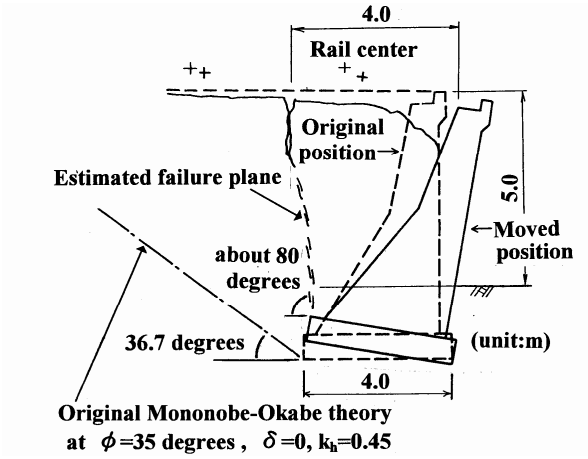

Figure 5. Residual displacement of wall and formation of failure plane (Tatsuoka et al, 1998)

3 TEST RESULTS AND DISCUSSION

3.1 *Failure pattern of models*

Fig. 4 shows the residual displacement of the wall and the residual deformation of the backfill, which were observed at the end of second shaking step. The major failure pattern of RW was sliding, and the formation of failure plane was clearly observed for Case 1, while it was not so clear for Case 2. This may be due to the smaller residual displacement of RW for Case2. Since the RW model was set on the iron plate with large resistance against sliding, the residual displacement of RW was smaller than that of Case 1, resulting in the small strain localization in the backfill. In this figures the location of failure plane obtained by M-O theory was also shown. The shear resistance angle φ (=51 degrees) and maximum base accelerarion were employed for applying M-O theory to obtain the angle of failure plane. It can be seen that the angle of observed failure plane measured from the horizontal direction is larger than that of M-O theory.

This behaivor in which the angle of failure plane is larger than that of M-O theory was consistent with the damaged

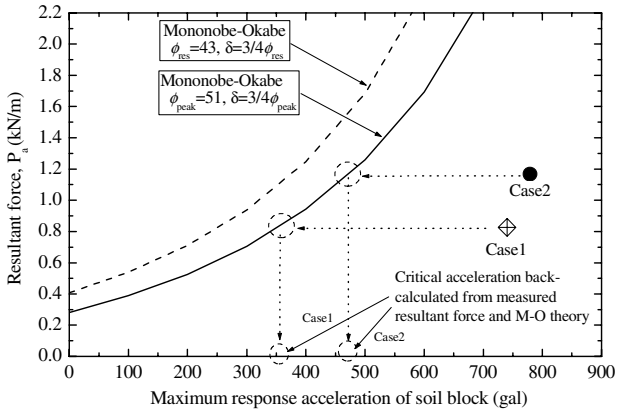

Figure 6. Relationship between resultant normal force and maximum response acceleration

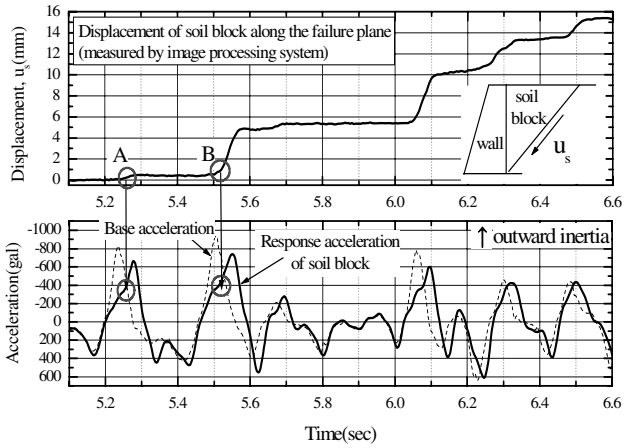

Figure 7. Time history of displacement of soil block along failure plane and acceleration

railway retaining wall after the Hyogoken-Nanbu earthquake (Fig. 5). These indicate that the location of failure plane was determined by the smaller acceleration not by the maximum acceleration of input motion. The failure plane probably started to form before the acceleration reached the maximum. In view of above, it became necessary to analyze the formation of failure plane during shaking in detail. This will be discussed later.

3.2 *Seismic earth pressure*

Relationship between the resultant force P_a acting normally on the facing from the backfill and the acceleration is shown in Fig. 6. Theoretical relationships based on the M-O theory are also shown in this figure. By considering that M-O theory derives the angle of failure plane by force equilibrium of soil block, maximum average acceleration which was obtained from the few accelerometers arranged in the soil block was employed for acceleration in this figure. The *Pa* values are evaluated by integrating normal and shear stresses measured with ten loadcells along depth of the facing, which include initial values measured before the start of shaking. This P_a value was defined when the response acceleration becomes peak state (on the negative side, inducing outward inertia force). This figure reveals that seismic earth pressure under large earthquake load is largely smaller than that obtained by M-O theory and this is mainly due to the effect of dynamic response of retaining wall which is not considered in M-O theory. This will also be discussed later.

It is noteworthy that the smaller seismic earth pressure was measured for Case 1 where the RW model was set on the steel plate having a smaller friction. This is because, when the inertia

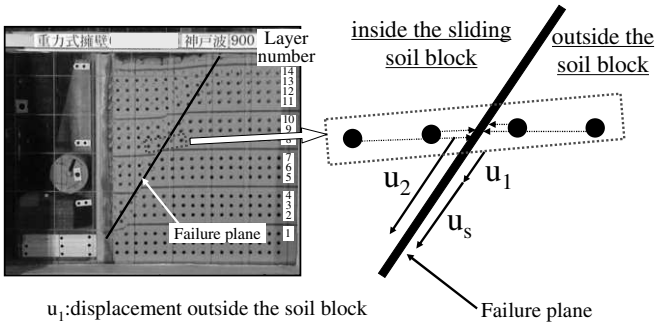

u_1:displacement outside the soil block

u_2:displacement inside the soil block

(u_1 and u_2 was obtained by extrapolating the displacement of two nearby targets along the failure plane)

$u_s=u_1 - u_2$ (average of relative displacement of u_1 and u_2 at all layer, 1-14 layer)

Figure 8. Displacement of soil block along the failure plane (u_s)

force was oriented toward the outward direction, the retaining wall moved outward more than the backfill, and the seismic earth pressure which should have been mobilized by the 'collusion' between the wall and the backfill did not increase after the outward displacement of retaining wall. That is why, the seismic earth pressure was smaller for Case1 with low seismic stability compared with that of Case 2, although the model was subjected to the exact same input motion. (Fig. 6)

Figs. 4 and 6 imply that the angle of failure plane and seismic earth pressure were determined not by the maximum acceleration but by the smaller acceleration, especially for Case 1. For example, the acceleration back-calculated by the measured angle of failure plane was around 350gal for Case1 and 470gal for Case2 (Fig. 6). Based on these results, it became necessary to investigate the following two points;

1. Deformation characteristic of backfill, particularly the moment of the formation of failure plane during shaking
2. The external force and resistance force acting on the retaining wall during shaking.

These two points will be discussed in the following two sections.

3.3 *Precise observation of the formation of failure plane*

Fig. 7 shows the time history of the displacement of soil block, u_s, along the failure plane and the response acceleration of soil block (Case1). This displacement was obtained by the relative displacement of a few targets in the vicinity of failure plane at each height. As schematically shown in Fig. 8, the displacement of inside and outside of failure plane was obtained by extrapolating the displacement of two nearby targets along the failure plane (u_1 and u_2), and u_s was the average of relative displacement of u_1 and u_2 at each layer, 1st to 14th layer in Fig. 8. It can be seen from Fig. 7 that u_s started to increase when the response acceleration of the soil block was around 350gal to 400gal (Point A for first large outward inertia and Point B for second inertia), which is smaller than the maximum of base acceleration (935gal). This indicates that the location of failure plane had already determined by the force equilibrium of soil block before the acceleration reached the maximum.

This may be because the external force acting on the RW reached to the maximum resistance force at this moment, resulting in the outward movement of RW. In summary, the acceleration in which the RW started to move outward determined the angle of failure plane.

3.4 *The external force and resistance force acting on RW during shaking*

Fig. 9 shows the time history of acceleration, wall displacement, external force and resistance force for Case 1. The external force was defined as the sum of horizontal inertia force and normal component of seismic earth pressure. Since the

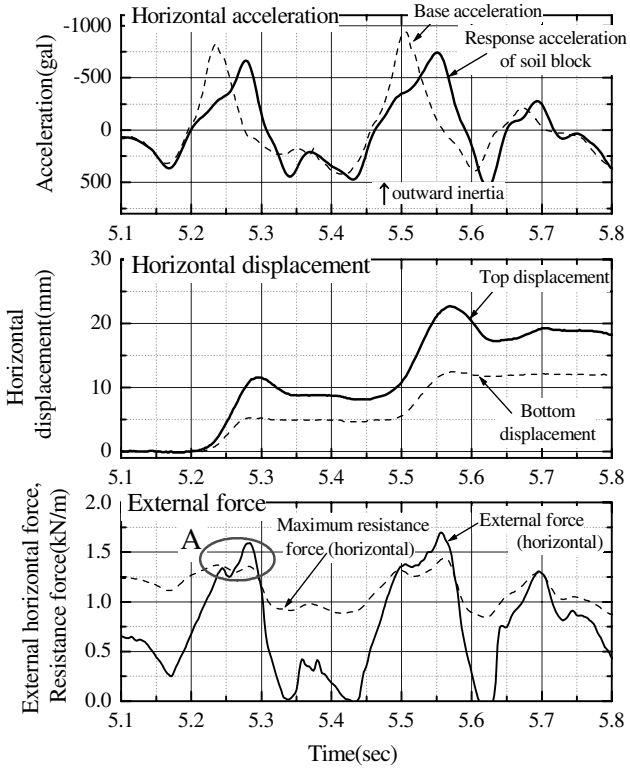

Figure 9. Time history of external force, maximum resistance force, displacement and acceleration

resistance force was not directly measured in this tests, it was obtained from the vertical load (total weight of RW and vertical component of seismic earth pressure) and maximum frictional angle of bottom of base footing. (34 degree for Case 1). It can be seen from this figure that the external force increased with the increase of acceleration until it reached to the maximum resistance force (Point A in Fig. 9). Even though the acceleration was still increasing, the external force cannot exceeds the maximum resistance force. The displacement of the wall was accumulated during this period. This acceleration (around Point A) can be defined as 'critical acceleration' of this retaining wall model. Similar tendency was also observed for Case 2 with larger friction angle of base footing, and the critical acceleration were around 400gal for Case1 and 500gal for Case2.

This critical acceleration agrees with the acceleration which was back-calculated from measured seismic earth pressure and M-O theory (Fig. 6). This indicates that the seismic earth pressure was determined mainly by critical acceleration.

3.5 New method to evaluate the seismic earth pressure under large seismic load using M-O theory

The shaking table model tests under large seismic load revealed that the seisimic earth pressure was largely smaller than that of M-O theory, and angle of failure plabe is larger than that of M-O theory. This is mainly due to the applicable limit of M-O theory where the dynamic response of retaining wall is ignored. On the other hand, it was found that the maximum earth pressure and the location of failure plane were determined around the critical acceleration.

In view of above, it should be suggested that the seismic earth pressure and the location of failure plane under large seismic load for practical design can be evaluated by applying the critical acceleration to the M-O theory. The critical acceleration can easily be obtained by static analysis of RW against sliding or rotation.

Since the M-O simply employs the maximum acceleration of input motion (around 700gal in the current design standard), it often derives an unrealistic large earth pressure under large seismic load. However, proposed method gives a reasonable earth pressure under large seismic load, which is depending on the seismic stability of RW. This method agrees with the past study by Watanabe (2003) and Nakamura (2005). Watanabe (2003) found that the seismic earth pressure varied with the seismic stability of RW. Nakamura (2005) pointed out that the maximum acceleration for applying the M-O theory to the practical design for RW should be around 400gal. This is based on the centrifuge model tests of gravity type retaining wall.

On the other hand, residual displacement of retaining walls is also affected by the seismic stability of walls, so the aforementioned method to evaluate the seismic earth pressure rationally should be applied to the design procedure with considering the residual displacement of the wall. It is necessary to establish a rational methods to evaluate the residual displacement of the retaining wall. This is one of the remaining issues for establishing the seismic design procedure of retaining wall.

4 CONCLUSION

In this study, a series of shaking table tests of RW under large seismic load were performed and the following conclusions were drawn.

1. Seismic active earth pressure acting on the retaining wall was largely smaller than that obtained by Mononobe-Okabe theory particularly under large seismic load.
2. Even though the earthquake load is large, only a small seismic earth pressure was measured for the low stability retaining wall. This is because the retaining wall moved outward by the inertia force more than the backfill.
3. It was found that maximum seismic earth pressure and the location of failure plane under large seismic load for practical design can be evaluated by applying the critical acceleration to the M-O theory. The critical acceleration can easily be obtained by stability analysis of RW against sliding or rotation.
4. This proposed method gives a reasonable earth pressure under large seismic load, which is depending on the seismic stability of RW. This value almost agrees with the experimental value in the past studies.
5. It became necessary to establish a rational methods to evaluate the residual displacement of the retaining wall. This is one of the remaining issues for establishing the seismic design procedure of RW.

REFERENCES

Tatsuoka, F., Koseki, J., Tateyama, M., Munaf., Y., and Horii, K. 1998. Seismic stability against high seismic loads of geosynthetic-reinforced soil rataining structures, *Keynote Lecture, Proc., 6th Int, Conf. on Geosynthetics*, Atlanta

Mononobe, N. and Matsuo, H. 1929. On Determination of Earth Pressure during Earthquake, *Proc. World Engineering Congress*, Tokyo, Vol. 9, pp.177-185

Nakamura, S. 2004. Study on rational seismic design of gravity type retaining walls. Doctoral thesis of University of Tokyo (in Japanese)

Okabe, S. 1924. General Theory on Earth Pressure and Seismic Stability of Retaining Wall and Dam, *Journal of Japan Society of Civil Engineers*, Vol. 10, No. 6, pp.1277-1323

Railway Technical Research Institute 2000. Railway Structure Design Standard for Foundations and Soil Retaining Structures (SI unit version), Maruzen, pp.130-135 (in Japanese)

Watanabe, K., Munaf, Y., Koseki, J., Tateyama, M. and Kojima, K. 2003. Behaviors of several types of model retaining walls subjected to irregular excitation, *Soils and Foundations*, Vol.43, No.5

Watanabe, K., Koseki, J., Tateyama, M. 2005. Application of High speed Digital CCD Cameras to Observe Static and Dynamic Deformation Characteristics of Sand, *Geotechnical Testing Journal*, ASTM, Vol.28, No.5, pp.423-435